Thermal Lensing Compensation in the Development of 30 fs Pulse Duration Chirped Pulse Amplification Laser System and Single-Shot Intensity-Phase Measurement

T. Imran[a,*] and M. Hussain[b]

[a]Department of Physics and Astronomy, College of Science, King Saud University, Riyadh, 11541, Saudi Arabia
[b]GoLP/Instituto de Plasmas e Fusão Nuclear, Instituto Superior Técnico, Universidade de Lisboa, Av. Rovisco Pais, 1049-001 Lisbon, Portugal

(Received June 27, 2016; in final form November 19, 2017)

We present 30 fs pulse duration home-made chirped pulse amplification Ti:sapphire laser system operating at a repetition rate of 1 kHz with 4.0 mJ pulse energy. The Ti:sapphire laser system with ~ 819 nm center wavelength has a long-cavity oscillator, four pass grating stretcher, 8-pass pre-amplifier, 4-pass post-amplifier and a double pass grating compressor. The Peltier coolers and thermal eigenmode post-amplifier are introduced to compensate the thermal lensing of the crystal in the amplifiers and to enhance the beam focusability on the crystal. The Strehl ratio and M^2 value measured by employing the Shack–Hartman wavefront sensor HASO4 to observe the spatial profile and beam quality. The most sensitive single-shot second harmonic generation frequency-resolved optical gating diagnostic technique is employed to characterize intensity and phase of the output compressed laser pulses.

DOI: 10.12693/APhysPolA.133.28

PACS/topics: lasers, laser optical systems: design and operation, nonlinear optics

1. Introduction

The thermal effects in the solid-state lasing materials have been under the extensive study and research [1, 2], and the challenging effect ascends; thermal lensing effects appeared due to the pump beam transverse intensity profile [3]. If the temperature in the crystal is non-uniform, it leads to spatial refractive index variations [4]. Consequently, thermal lens is formed. The capability of laser pulse was significantly affected due to thermal lens effect which results in the wavefront distortion [5]. The temperature variations in the Ti:sapphire crystal, the heat distributions and the heat dissipation of absorbed pulse energy have been simulated [6], and steady state solution analyzed [7]. The thermal lens effect results in the mismatch of modes between the lasing material surface and wave-front of the beam which enhanced the photon shot noise [8]. Various research groups have put their efforts to reduce the optical absorption in sapphire to minimize the thermal lensing effect [9, 10].

The femtosecond laser pulses with terawatt and petawatt peak powers obtained by chirped pulse amplification (CPA) technique [11]. Such high peak power laser systems are used to study high harmonics generation, white light continuum generation, plasma and optical field ionization [12–14]. A rapid advancement in the development of high-average-peak power CPA laser systems [11, 14–16] has been observed in recent years. However, many technical issues related to development and characterization needs to be addressed. Most important is thermal distortion and thermal lensing in a kHz repetition rate Ti:sapphire CPA system because the strong pump power in amplifiers induced the thermal effect in the amplifying crystal such as the distortion in the amplified pulse wavefront, miss-match of modes which results in the phase distortion and consequently decreases the efficiency of amplification. In CPA based laser system, residual phase errors and gain narrowing are two restriction aspects of generating 20 fs pulses. A higher gain leads to narrow the pulse spectrum in preamplifier due to high amplification; gain narrowing is the major reason for pulse broadening in femtosecond laser systems. The phase distortion appears due to inaccurate compensation of dispersion in compressors which is because of supplementary material dispersion in multipass amplifiers. The one way to compensate the thermal distortion and thermal lensing effect is to introduce converging lens after each pass after the amplifying crystal which is not realistic. The other method which we have adopted by employing the para-axial Gaussian beam propagation in the amplifier resonator and measure its eigenmode. As after one round trip, eigenmode reproduces itself which is equivalent to reimaging of pulses after every pass in the multipass amplifier. Therefore, when the input beam matched with the eigenmodes of the post-amplifier, the thermal lensing effect does not influence the output beam of the post-amplifier. The length of the multipass amplifier for the eigenmode propagation depending on the average pump power was described [17]. The reduction in the thermal lensing effect and thermal distortion in the Ti:sapphire based laser system has been maintained by employing the water cooling [18, 19] and cryogenically cooled [20]. Along with the thermal compensation, the phase fluctuations and pulse duration required to be

*corresponding author; e-mail: timran@ksu.edu.sa

measured accurately. For this purpose, the second harmonic generation (SHG) frequency-resolved optical gating (FROG) diagnostic technique employed [21–25].

In this article, we present development and intensity-phase characterization of Ti:sapphire-based CPA laser system operating at 1 kHz repetition rate having 4.0 mJ pulse energy at ~ 30 fs pulse duration. The thermal lens effect and thermal distortion were compensated by employing the Peltier coolers and thermal eigenmode in the post-amplifier. The wavefront, beam quality, the Strehl ratio and M^2 value measured by employing the Shack–Hartman wavefront sensor HASO4 (Imagine Optic). The intensity-phase characterization was carried out by the SHG-FROG diagnostic technique.

2. CPA laser system

A Ti:sapphire CPA laser system operating at the repetition rate of 1 kHz has an oscillator, grating stretcher, multi-pass pre-amplifier, post-amplifier and double pass grating compressor. Femtosecond laser pulses obtained through a prism dispersion controlled Ti:sapphire oscillator in the long-cavity arrangement running at the repetition rate of 27 MHz [26]. The amplified spontaneous emission (ASE) can be reduced in CPA laser system by employing long-cavity oscillator as a front end so that the number of passes in amplifier could be reduced [26]. The high contrast pulse can be selected in CPA Ti:sapphire system by keeping the long interval between the pulses. The output pulse of long-cavity oscillator stretched to ≈ 220 ps in the Offner triplet, an aberration-free reflective type stretcher [27], having 1400 grooves/mm grating. Pulse is made to pass through the Faraday rotator to block the back reflection and backward ASE from the amplifier.

The pulse then were sent to 8-pass pre-amplifier, the detailed scheme of CPA system is shown in Fig. 1a. The two focusing mirrors and three flat mirrors of 90 cm radius of curvature used in amplifier with two curved mirrors arranged in the confocal geometry. A Nd:YLF frequency-doubled Q-switched pump laser (Darwin, Quantronix Inc.) with pulse energy of 10 mJ employed as a pump source in pre-amplifier. The first curved mirror focused the laser beam into the crystal and the second curved mirrors collimated the beam again and sent to flat mirrors. The pulse train is extracted from the pre-amplifier after four passes and selected by the Pockels cell at a 1 kHz repetition rate. The extracted pulse directed to pre-amplifier to complete the remaining 4 passes where energy raises up to 1.2 mJ. The output pulses from pre-amplifier are directed to post-amplifier after passing through the second Pockels cell, which minimizes the ASE emerges out from the pre-amplifier and improves the contrast ratio. The Ti:sapphire crystal of post-amplifier pumped by 20 mJ and 30 mJ laser pulses from a Q-switched Nd: YLF laser (Falcon, Quantronix Inc.) and a residual pump 1st Nd:YLF laser respectively. Finally, the output pulse energy approaches to 7.2 mJ at the output of the post-amplifier [28].

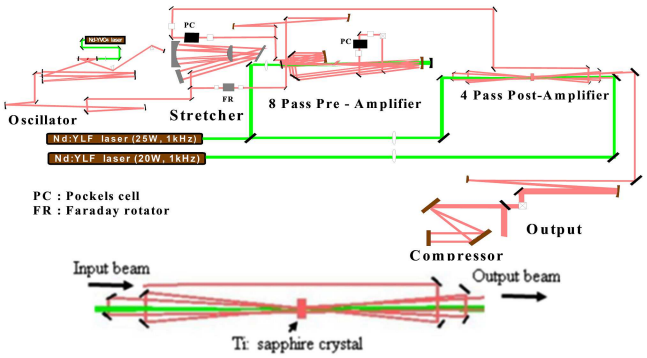

Fig. 1. Diagram of 1 kHz repetition rate Ti:sapphire CPA laser system (top) ans thermal eigenmode 4-pass post-amplifier (bottom).

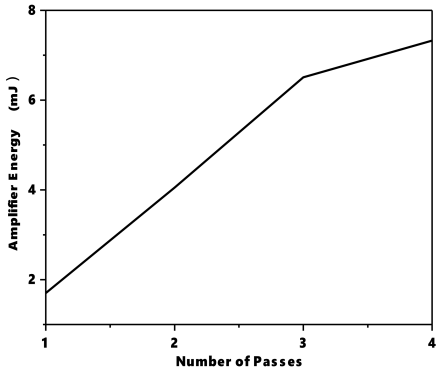

Fig. 2. Number of passes vs. output pulse energy measured after each pass in post-amplifier.

When a high pump power is used as a pump source, thermal lensing arises which was induced by heating in the amplifier crystal. Because of thermal lensing effect, optical damage and mismatching of modes between the pump and amplified beam appeared in succeeding passes. The beam focusability was reduced because of higher thermal aberration which is due to characteristics of thermal lensing outside the pumped area in the crystal. Therefore, for proper amplification efficiency and good beam quality, one must compensate the thermal lensing [29, 30]. The crystal cooling and thermal eigenmode in post-amplifier [29, 17] are employed to compensate the thermal lensing. We installed the Peltier cooler to lower the temperature of the crystal up to $\approx 40\,^{\circ}$C. The Peltier cooler was attached to the copper block on which the crystal mounted. By cooling the Ti:sapphire crystal, thermal conductivity increases and change in refractive index per unit temperature decreases which results in the decrease in thermal lensing [17]. Thermal eigenmode introduced in the 4-pass post-amplifier (Fig. 1b) to keep the beam size of the amplified laser pulses on the crystal, to get rid of thermal lensing effect. The measured output pulse energy per pass of the post-amplifier is as shown in Fig. 2. As it is evident from the plot, the pulse energy increases linearly with the number of passes through the amplifier, because the cavity losses super-

seded by the amplification. The pulse energy grows up as a function of number of passes in the cavity, but on enhancing the number of passes, the pulse energy gains saturation value and falls with further increase of passes in the multi-pass amplifier due to beam divergence and cavity losses. Therefore we limited the post amplifier to 4-pass.

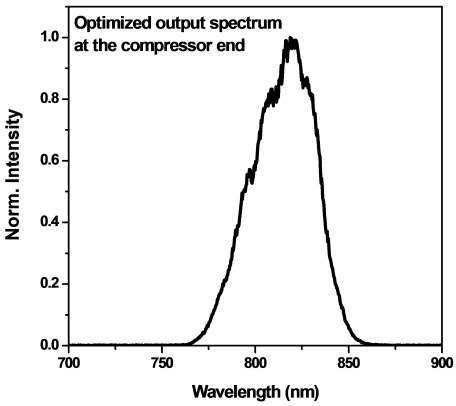

Fig. 3. Compressed output spectrum.

The output pulses of the post-amplifier are made to double pass through a pair of parallel gratings having 1480 grooves/mm. To eliminate the thermal distortion and to avoid the optical damage on the gratings, a pair of concave/convex mirrors were used to expand the beam diameter to 25 mm. Pulses of 4.0 mJ obtained at the output of the compressor with throughput efficiency of $\approx 60\%$. The 45 nm broad output spectrum at the compressor end is shown in Fig. 3. The wavefront measurement carried out by employing Shack–Hartman wavefront sensor HASO4 (Imagine optic). The Strehl ratio which describes the quality of the image is also obtained from the point spread function. The Strehl ratio allows us to compare the actual maximum intensity on the focal plane to a perfect intensity free of aberrations. The Strehl ratio measured by using the Shack–Hartman wavefront sensor HASO4 is 0.930 and M^2 value is 1.49 which shows the stability of phase and nice beam quality and less divergence.

3. Intensity-phase characterization of CPA laser system

The FROG diagnostic technique used for the characterization of ultrafast laser pulses in frequency and time domains simultaneously, which can also be described as a spectrally resolved autocorrelation measurement [22]. We employed the sensitive single-shot second harmonic generation (SHG) FROG diagnostic technique to characterize this laser system. In this technique compressed pulse after the compressor splits into two identical pulses by using 50-50 beam splitter, these pulses were line-focused by using a cylindrical mirror; the focused pulses then recombined in a nonlinear beta barium borate (BBO) crystal of thickness 100 μm. The schematic of single shot SHG-FROG shown in Fig. 4.

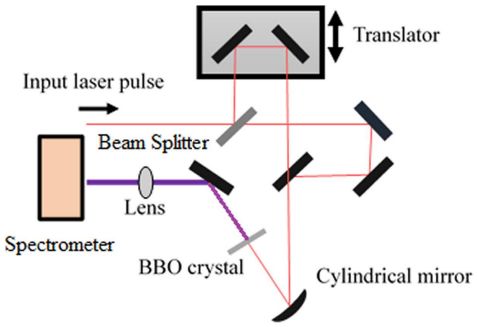

Fig. 4. Diagram of single-shot FROG diagnostic to characterize the laser pulses.

The split beams are line focused with a small angle of 2° to accomplish single-shot FROG configuration. This small angle beam overlapping geometry in the nonlinear crystal reduces the phase mismatching, but the measurable temporal range shortened. The experimental scheme of FROG setup is shown in Fig. 5. The output pulse from the nonlinear crystal is spectrally-resolved by a grating with 150 grooves/mm and captured by a CCD camera, which is called the FROG trace or image. For the analysis of the FROG trace, commercial FROG (Femtosoft Inc.) software was used. The FROG software algorithm uses the experimental input data. By starting with an Initial guess, a closer guess generated through the algorithm of iterative Fourier transform which approaches the correct electric field. After running number of iterations, the FROG error shows the reliability of the retrieval process [23]. This single-shot FROG trace or image is a two-dimensional spectrogram, which has a delay time axis and a wavelength axis. By using the FROG algorithm, phase and intensity profiles of test pulse can be retrieved from the experimental FROG traces that may provide essential information about the test pulse in terms of intensity and phase profiles [24].

At the compressor end of CPA system, the efficiency of a laser pulse was optimized by adjusting the gratings separation and incident angle into the grating. A two-dimensional FROG trace retrieved from the measured trace by running number of iterations using FROG software. From the two-dimensional FROG trace, retrieved temporal and spectral evolution of the compressed pulse plotted, which reveals the spectral and temporal phase variations. We observe that the full-width half-maximum (FWHM) of retrieved temporal profile is $\approx$ 30 fs with relatively flat temporal phase variations, which changes from 1 rad peak to peak which is shorter than reported earlier [17, 29] as shown in Fig. 5.

Similarly, the retrieved spectral profile indicates that the phase distortion is less than 1 rad over the bandwidth of $\approx$ 70 nm. There is a reasonably good agreement of bandwidth and shape of retrieved and measured spectrum (Fig. 6, spectral profile) with considerably small FROG error $G = 0.002835$ [26–31], where G is a root mean square error between the experimental and retrieved FROG trace. The information retrieved from

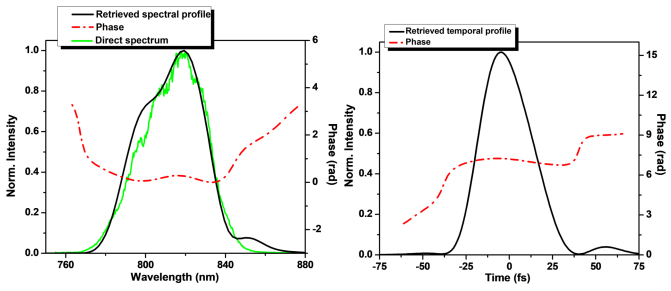

Fig. 5. (left) Retrieved spectral profiles of amplified laser pulses (left) and temporal profiles of amplified laser pulses (right).

the pulse becomes reliable if FROG error is below than the noise level of the experimental trace [22–24]. These retrieved profiles completely characterize the 1 kHz femtosecond laser pulses.

4. Conclusion

A femtosecond Ti:sapphire-based CPA laser with 4.0 mJ energy per pulse, having ≈ 30 fs pulse duration operating at 1 kHz repetition rate has been described and characterized by single shot SHG FROG technique. The long-cavity oscillator was used as the front end of CPA system because of broadband spectrum, low ASE and the long interval between pulses. The Peltier coolers were used to cool down the Ti:sapphire crystal for the compensation of thermal lensing while thermal eigenmode is introduced in the post-amplifier to keep the beam size of the amplified laser pulses on the crystal and to avoid the thermal lensing effects. The Strehl ratio and M^2 values, 0.930 and 1.49, respectively, were measured by the Shack–Hartman wave-front sensor which is the clear signature of the stability of spatial profile and thermal lensing compensation. Finally, sensitive SHG-FROG single-shot technique was employed to characterize the spectral and temporal profiles of CPA laser system.

Acknowledgments

The authors acknowledge the part of this research was carried out at Korea Advanced Institute of Science and Technology (KAIST), South Korea. One of the authors would also like to greatly acknowledge the support of Prof. Dr. Nam Chang Hee and senior fellow Dr. Jae Hee Sung.

References

[1] U.O. Farrukh, A.M. Buoncristiani, C.E. Byvik, *IEEE J. Quantum Electron.* **24**, 2253 (1988).

[2] M.E. Innocenzi, H.T. Yura, C.L. Fincher, R.A. Fields, *Appl. Phys. Lett.* **56**, 1831 (1990).

[3] C. Pfistner, R. Weber, H.P. Weber, S. Merazzi, R. Gruber, *IEEE J. Quantum Electron.* **30**, 1605 (1994).

[4] J. Tapping, M.L. Reilly, *JOSA A* **3**, 610 (1986).

[5] J. Sung, T. Jeong, S. Lee, T. Yu, I. Choi, J. Lee, *J. Kor. Phys. Soc.* **55**, 495 (2009).

[6] A. Börzsönyi, R.S. Nagymihály, K. Osvay, *Laser Phys. Lett.* **13**, 015301 (2015).

[7] G. Wagner, V. Wulfmeyer, A. Behrendt, *Appl. Opt.* **50**, 5921 (2011).

[8] P. Hello, J.Y. Vinet, *Phys. Lett. A* **178**, 351 (1993).

[9] T. Tomaru, T. Suzuki, S. Miyoki, T. Uchiyama, C.T. Taylor, A. Yamamoto, T. Shintomi, M. Ohashi, K. Kuroda, *Clas. Quant. Grav.Â* **19**, 2045 (2002).

[10] D. Blair, F. Cleva, C.N. Man, *Opt. Mater.* **8**, 233 (1997).

[11] T.J. Yu, S.K. Lee, J.H. Sung, J.W. Yoon, T.M. Jeong, J. Lee, *Opt. Expr.* **20**, 10807 (2012).

[12] T. Imran, M. Hussain, G. Figueira, *Laser Phys. Lett.* **13**, 066101 (2016).

[13] V.P. Kandidov, O.G. Kosareva, I.S. Golubtsov, W. Liu, A. Becker, N. Akozer, C.M. Bowden, S.L. Chin, *Appl. Phys. B Lasers Opt.* **77**, 149 (2003).

[14] H.G. Roskos, M.D. Thomson, M. Kreß, T. Loffler, *Laser Photon. Rev.* **1**, 349 (2007).

[15] J.H. Sung, S.K. Lee, T.J. Yu, T.M. Jeong, J. Lee, *Opt. Lett.* **35**, 3021 (2010).

[16] Y. Chu, X. Liang, L. Yu, Y. Xu, L. Xu, L. Ma, X. Lu, Y. Liu, Y. Leng, R. Li, Z. Xu, *Opt. Expr.* **21**, 29231 (2013).

[17] R. Salin, C.L. Blanc, J. Squier, C. Barty, *Opt. Lett.* **23**, 718 (1998).

[18] G. Matras, N. Huot, E. Baubeau, E. Audouard, *Opt. Expr.* **15**, 7528 (2007).

[19] I.H. Baek, H.W. Lee, S. Bae, B.H. Hong, Y.H. Ahn, D.I. Yeom, F. Rotermund, *Appl. Phys. Expr.* **5**, 032701 (2012).

[20] R. Nagymihály, P. Jojart, A. Borzsonyi, K. Osvay, in: *High Intensity Lasers and High Field Phenomena*, Optical Society of America, HS3B-4, 2016.

[21] K.H. Hong, Y.H. Cha, C.H. Nam, J.D. Park, *J. Kor. Phys. Soc.* **33**, 315 (1998).

[22] R. Trebino, K.W. Delong, D.N. Fittinghoff, J.N. Sweetser, M.A. Krumbügel, B.A. Richman, D.J. Kane, *Rev. Sci. Instrum.* **68**, 3277 (1997).

[23] T. Imran, M. Hussain, G. Figueira, *Microwave Opt. Technol. Lett.* **59**, 3155 (2017).

[24] K.H. Hong, J.H. Sung, Y.S. Lee, C.H. Nam, *Opt. Commun.* **213**, 193 (2002).

[25] Y. Takao, T. Imasaka, Y. Kida, T. Imasaka, *Appl. Sci.* **5**, 136 (2015).

[26] J.H. Sung, K.H. Hong, Y.H. Cha, C.H. Nam, *Jpn. J. Appl. Phys.* **41**, L931 (2002).

[27] G. Cheriaux, P. Rousseau, F. Salin, J. Chambaret, B. Walker, L. Dimauro, *Opt. Lett.* **21**, 414 (1996).

[28] J.H. Sung, K.H. Hong, C.H. Nam, *J. Kor. Opt. Soc.* **7**, 135 (2003).

[29] C. Le Blanc, E. Baubeau, F. Salin, J.A. Squier, C.P.J. Barty, C. Spielmann, *IEEE J. Select. Top. Quant. Electron.* **4**, 407 (1998).

[30] C.G. Durfee, S. Backus, M.M. Murnane, H.C. Kapteyn, *IEEE J. Quant. Electron.* **4**, 395 (1998).

[31] D.J. Kane, R. Trebino, *IEEE J. Quant. Electron.* **29**, 571 (1993).